Investigation of a Supersonic Surface Jet—Hypersonic Flow Interaction with Axial Symmetry

RAYMOND P. SHREEVE*
Boeing Scientific Research Laboratories, Seattle, Wash.
AND
GORDON C. OATES† AND HARLOW G. AHLSTROM‡
University of Washington, Seattle, Wash.

An experimental investigation of axially symmetric slot injection of a supersonic jet into a hypersonic stream has been carried out. A cone of 5° half angle was constructed in such a way that jet injection at six different angles could be provided. The throat areas and exit areas of the slots were the same in all cases, and provided a nominal jet Mach number of (2)‡. The freestream Mach number was 6 in all cases. The boundary layer at the point of injection was fully turbulent. Optical investigations were made, and surface pressure distributions were obtained. Stagnation temperature and stagnation pressure surveys were made downstream of the injection point, the results being reduced by digital computer to provide mass flux profiles. The results indicate that three basic types of interaction occur depending on the angle of the jet. Equations describing the displacement of the dividing streamline for each of the three interaction types are established empirically, and the streamline displacement is compared to separation and shock displacement scales. Jet mass entrainment is also examined. It is tentatively concluded that jets of intermediate angle hold promise of advanced propulsion applications, while jets at small angles provide stable films, as necessary in thermal protection applications.

Nomenclature

A = area
A^* = jet nozzle throat area (= 0.1964 in.^{2})
A_j = jet nozzle exit area (= 0.2201 in.^{2})
A_ψ = area contained between the dividing streamline and the cone surface in a plane normal to the cone axis
h_j = equivalent jet exit height defined by $A_j = 2\pi h_j r_j$ (= 0.0572 in^2)
$\dot{m}$ = mass flow rate
$\dot{m}_{en}$ = mass flow rate entrained by the jet up to the measurement plane
$\dot{M}$ = total mass flow rate contained between the cone surface and $y = y_e$
p = static pressure
p^t = stagnation pressure
r = distance from the cone axis
r_j = radius of the cone surface at the jet upstream edge (= 0.6124 in.)
R = r/r_j
S = the "jet strength"; defined as $S = p_j^t/p_c$
u = velocity in the direction of the cone surface
x = distance along the cone surface from the upstream edge of the jet
X = x/h_j
y = distance above the surface measured normal to the cone axis
Y = y/h_j
θ = jet angle measured with respect to the cone surface
ρ = density
γ = ratio of specific heats
Δ = total displacement of the outer flow by the jet
Γ = $[(\gamma + 1)/2]^{(\gamma+1)/2(\gamma-1)}$

Subscripts

c = cone surface conditions for zero blowing
e = edge of mixing layer
$i.i.s.$ = internal injection shock wave
is = isentropic
j = jet
$n.s.$ = normal shock
pl = "plateau" value
ψ = dividing streamline
f = freestream

Introduction

THIS paper describes the results of a recent investigation of a two-dimensional surface jet—hypersonic flow interaction carried out using a slender conical surface with a fully turbulent boundary layer.[1]

Earlier investigations of the two-dimensional problem have been concentrated on the generation of side force for aerodynamic control. With few exceptions,[2] investigators have devoted their efforts to the prediction and measurement of the "amplification factor" for the special case of a highly underexpanded sonic jet normal to the surface. This aspect was recently reviewed by Werle.[3] In other applications, to hypersonic ramjets[4] and lifting propulsive bodies[5] for example, the jet-flow interaction must be understood first in greater generality, and then in greater detail, since it must be optimized within the aerodynamic and propulsion design of the vehicle. The transverse scale of the interaction (or "jet penetration"), the surface pressure distribution, and the mixing behavior must be known as a function of all the independent parameters of the jet. Since, in general, the flowfield can contain significant regions of separated flow, and since it can be argued that basic changes in the flow structure will occur as the jet parameters are varied, experiments should precede the formation of mathematical models. This approach, which was followed successfully by Finley[6] in dealing with the problem of a jet from a body opposing a supersonic flow, is the one adopted here.

Only recently have experiments been reported in which surface jet-flow interaction was studied in a fully axisymmetric geometry.

Received February 8, 1971; revision received November 22, 1971. This research was supported by The Boeing Company through the corporate office of the Flight Sciences research program, under the direction of A. Goldburg. The first author further acknowledges The Boeing Company for its support through the Graduate Study Program.

Index categories: Hypersonic Airbreathing Propulsion; Jets, Wakes, and Viscid-Inviscid Flow Interactions; Supersonic and Hypersonic Flow.

* Staff Member, Flight Sciences Laboratory; presently Visiting Associate Professor, Department of Aeronautics, Naval Postgraduate School, Monterey, Calif. Member AIAA.

† Professor, Department of Aeronautics and Astronautics. Associate Fellow AIAA.

‡ Professor, Department of Aeronautics and Astronautics. Member AIAA.

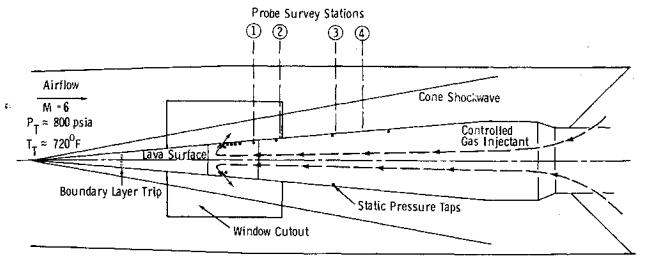

Fig. 1 Schematic of the experiment

This choice avoids the many difficulties which attend the generation of planar two-dimensional flows containing separated regions. Simpkins[7] used a conical surface and a jet from a circumferential slot in a hypersonic shock tunnel. Surface pressure and heat-transfer measurements were obtained at a Mach number of 13.5 and at Reynolds numbers less than 10^6. The boundary layer was laminar and the flowfield was wholly in the laminar viscous interaction regime. In Ref. 8, a circumferential slot around a cylindrical surface was used for an investigation directed at film cooling effects of surface jets. In the latter experiments, the slot width was small compared to the turbulent boundary-layer thickness.

The present investigation began by considering the dimensionless parameters which govern the flowfield. Given the constraint of the investigation, that freestream conditions remain fixed, physical arguments suggested two parameters to be controlling. The two parameters (the jet to surface pressure and the jet angle) were varied over a wide range and a detailed determination of the flowfield was made at each operating point. The combination of a very small stagnation temperature probe with fast response[9] and an impact pressure probe, permitted the measurement of the distribution of mass flux, from which the dividing streamline and edge of the mixing layer were determined.

The investigation defined different regimes for the jet interaction flowfield and showed the basic changes in properties which occur in going from one regime to another. Correlations were found for the dividing streamline displacement, and the entrainment into the jet was shown to depend critically on the jet-surface boundary-layer interaction.

Description of the Experiment

The experiment was designed to have a completely axisymmetric geometry. A long 5° cone surface and a circumferential slot were used to avoid the difficulties of the planar two-dimensional geometry while providing the required symmetry and a known reference flowfield.

The parameters chosen for the investigation were the jet to surface pressure ratio and the jet angle. These are the parameters which govern the initial angle of the jet streamline as it leaves the upstream corner for a given jet Mach number, and will therefore initiate basic changes in the geometry of the flowfield. Also, controlling the angle of the jet was a means of controlling the normal component of the jet momentum without simultaneously requiring changes in other dimensionless groups. The freestream flow was held constant throughout the experimental investigation.

Table 1 Diagnostic techniques and information given

1. Optical	
a) Spark shadowgraph (high contrast)	Location of upstream separation; Upstream separation shock wave; Main injection shock wave; Trailing (recompression) shock wave; Edge of mixing layer at low-blowing rates
b) $\frac{1}{60}$th sec schlieren photograph	Shock wave structure within the jet
c) Oil flow	Location of downstream separation
2. Surface pressure taps	Pressure distribution downstream of the jet
3. Probe surveys	Complete flow profiles at four axial stations downstream of the jet, yielding: 1) dividing streamline location (y_ψ); 2) edge of mixing region (y_e); 3) mass entrainment; 4) displacement thickness of the mixing region outside the dividing streamline

The general arrangement of the experiment is shown in Fig. 1. The investigation was carried out using a 6 in. axisymmetric Mach 6 wind tunnel operated nominally at a stagnation pressure of 800 psi and a stagnation temperature of 720°F. Details of the wind-tunnel design, operation, and calibration are contained in Ref. 1. The injected air was supplied at 70°F with a stagnation pressure range of approximately 6–130 psia. The corresponding range of the "jet strength" S was approximately 12–250. The 5° conical blowing model, 18 in. long, was held on the axis of the wind tunnel such that the peripheral jet, 7 in. from the tip, was positioned in the 4 in. windows. The model was constructed in sections to allow 6 jets at angles 5, 10, 20, 45, 90, and 120° to be tested. Each jet was designed to have the same throat area and exit area and to give an exit Mach number equal to (2)[1]. It should be noted here that the "exit area" refers to that area obtained by constructing a line perpendicular to the upstream jet passage wall from the exit edge to the downstream jet passage wall. This line cylindrically swept through 360° gives the exit area. Since the passage surfaces are not parallel, the surface slot area is only approximately this area times cosec θ. A boundary-layer trip was located $3\frac{1}{2}$ in. from the cone tip, the purpose of which was to stabilize the location of transition to be symmetrical around the cone. In the absence of the trip, transition occurred naturally well ahead of the jet. The surface upstream of the jet was constructed

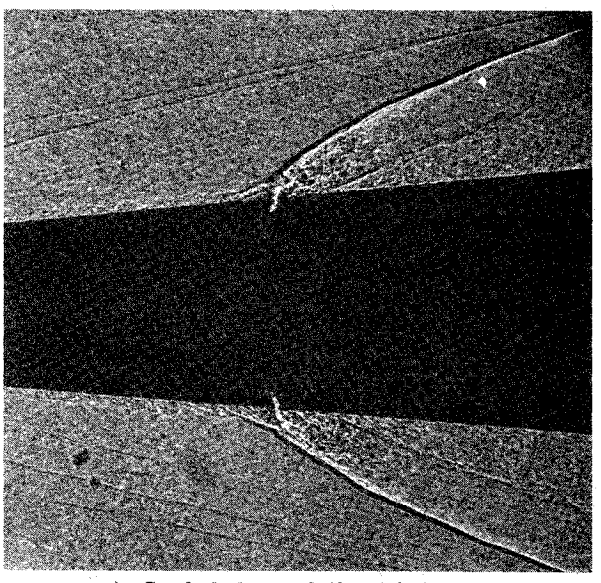

a) **Spark shadowgraph** ($\theta = 45°$, $S = 40$)

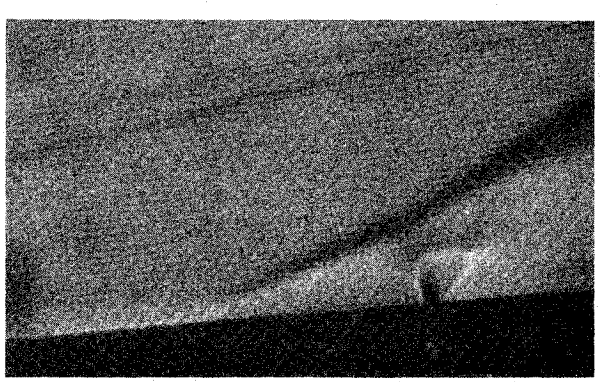

b) $\frac{1}{60}$**th sec schlieren** ($\theta = 90°$, $S = 42$)

Fig. 2 Examples of optical records.

of lava to ensure adiabatic flow up to the jet nozzle exit. Static pressure taps were located in the surface downstream of the jet.

The traversing probe system carried an impact tube closely adjacent to a miniature stagnation temperature probe. The fine wire thermocouple probe was developed as a preliminary study for the present application and is reported in Ref. 9. A complete description of the probe system, the data recording and reduction techniques, and a discussion of the accuracy achieved is found in Ref. 1. A summary of the diagnostic techniques employed and the derived information is given in Table 1.

Results: Regimes of the Surface Jet–Flow Interaction

From the optical evidence, and from probe results, the flowfields identified with the six jet angles investigated fell into three groups. The 5°, 10°, and 20° jets, referred to as "shallow" jets gave interaction structures which were characterized by the fact that the jets turned downstream through oblique shock waves and remained supersonic. The 90 and 120° jets, referred to as "near-normal" jets were characterized by the fact that their structure contained strong shock waves through which the flow became subsonic before turning downstream. These jets were fully separated from the surface both upstream and downstream of the jet exit. The 45° jet had features observed in both the shallow jets and the near-normal jets, and is best characterized as transitional. At low pressures, the interaction structure was similar to the near-normal jets; whereas, at high pressures, the downstream structure became similar to that of the shallow jets. The transition in the downstream structure from the near normal to the shallow characteristic pattern was accomplished by a change in the dependence of all measured quantities, but a sudden change in the wave structure was not observed. The results of the optical observations will be described according to the classification shallow, near normal, and transitional.

Two illustrative examples of shadowgraph and schlieren photographs of jet-flow interactions are given in Fig. 2. The spark shadowgraph (Fig. 2a) shows clearly regions of turbulence, while the focused schlieren photograph (Fig. 2b) shows the shock structure within the jet.

Underexpanded Shallow Jet

In Fig. 3a the structure of the highly underexpanded shallow jet is shown in a sketch which is based on the evidence of photographs such as those in Figs. 2a and 2b, oil flow observation and surface pressure measurements. The interaction at the upstream edge of the jet generates curved shock waves both inside the jet layer and in the outer flow. They will be referred to as the internal and external injection shock waves, respectively. The edge of the turbulent layer is initially close to the external injection shock wave and the dividing streamline will lie between the turbulent edge and the internal shock waves. The expansion fan from the downstream edge of the jet is at a small angle to the jet direction because the flow approaching the corner is at a high Mach number. The recompression shock wave appears as a reflection of the internal injection shock wave from the surface. Oil flow observations revealed the presence of flow separation in this region. Careful measurements indicated that separation originated upstream of the reflection point where a second shock wave is observed to originate at the surface. Thus, a structure somewhat similar to that of a shock wave reflecting from a laminar boundary layer was observed.

A special case of the shallow jet interactions is that wherein the pressure existing at the exit of the upstream edge of the slot is just that necessary to equal the pressure behind the external shock wave, without deflection of the injected flow. This condition is termed the "matched jet," and generally corresponds to a rather small injection rate. Extensive tests have shown for the shallow jets that, as the injection pressure is increased above the "matched" value, the structure within the jet remains qualitatively unchanged. As the injection pressure increases, the external and internal shock waves gradually increase in strength, and the recompression shock wave is moved further downstream. The only added feature is the appearance and gradual growth with increasing pressure of a region of separation upstream of the jet.

Underexpanded Near-Normal Jet

The structure observed for jets at 90° and 120° to the surface was qualitatively consistent with published observations of planar jets normal to the surface. Fig. 3b shows the main features of the flowfield. Little change was observed in the over-all flow pattern over a wide range of injection pressures. From the photographs, measurements of the length of the upstream separation region, the separation shock wave angle, and the displacement above the surface of the "Mach disk" were made. These measurements are discussed later.

Jet at 45°

Figures 3c and 3d illustrate the transitional behavior of the jet at 45°. The upstream region is similar to the near-normal jets. There is a large region of separation upstream of the jet, and the upstream separation shock and the external injection shock merge with little difference in curvature.

The region downstream of the jet, however, changes as S is increased. At $S = 40$ and below, only one recompression shock wave is evident and the static pressure distribution downstream is qualitatively similar to the near-normal jets. Above $S = 100$ the pattern of shock waves downstream is similar to that for the shallow jets, and the static pressure distributions become correspondingly similar also.

The transition of the downstream structure involves a progressive shrinking of the downstream separated region as the

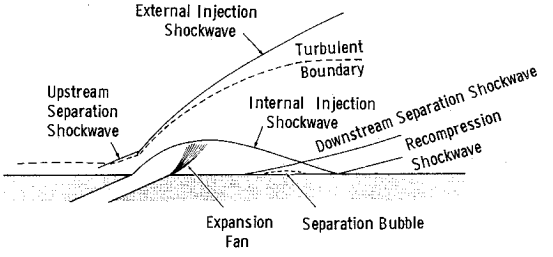

a) Shallow jet

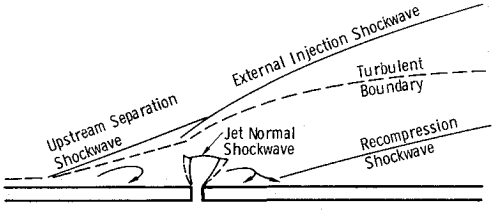

b) Near-normal jet

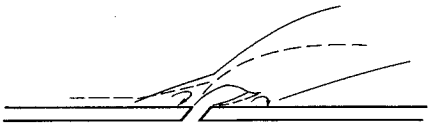

c) Transitional jet (low pressure)

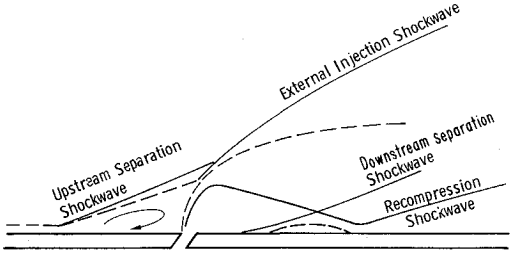

d) Transitional jet (high pressure)

Fig. 3 Observed flow structure for jets of different angles.

flow from the downstream edge expands further and further around the corner. When the jet pressure is sufficiently high, the flow completes a centered expansion through a 40° angle. Then the shock wave, which at low pressure was an internal shock typical of an underexpanded plume structure, becomes the downstream separation shock wave. The transition appeared to be smooth judging from the optical records. However, the surface pressure downstream shows a distorted profile at $S = 101$,[1] and there is a sharp increase in the scale of the upstream separation. Also, between $S = 110$ and $S = 164$ there is a change in the behavior of all properties derived from probe measurement. Thus, associated with the transition there is a change in the jet structure which needs further investigation.

Detailed Experimental Results

Surface Pressure Distributions

The pressure distributions as a function of the nondimensional downstream distance are shown for examples of each type of behavior in Fig. 4. The pressure immediately downstream of the near-normal jets is characteristic of a wake-like separated region such as exists behind a downstream facing step. Through the region of separation, the pressure is nearly constant and the pressure is not very sensitive to jet strength (or equivalently, step height). There is a definite, though small, difference in the measurements for the 90° and 120° jets at similar strength.[1] In contrast, the characteristic feature of the shallow jets is that ahead of the separation and recompression shock waves the flow is expanding and the pressure is falling.

The measurements for the jet at 45° show the transition from the wave-like distribution of the near-normal jets at $S = 37.8$, to a distribution characteristic of the shallow jets at $S = 158$.

Surface pressure measurements indicated that within the length available downstream of the jet ($X = x/h_j = 98.6$), the pressure had not yet readjusted to the undisturbed surface value, even for the lowest jet strength. Downstream of the recompression shock wave, and the associated peak pressure, the pressure decreases to a value less than the undisturbed cone pressure and then very slowly increases toward the undisturbed cone pressure. This behavior was verified by plotting the surface pressure recorded at each of three downstream locations as a function of the jet strength.

Dividing Streamline Displacement

The probe surveys indicated that streamwise property gradients were substantially smaller than property gradients normal to the stream surface. It was, hence, expected that correlations could best be obtained in terms of the transformed normal coordinate RY_ψ, which itself results from applying a Mängler transformation.[10]

With one exception the variation in the dividing streamline displacement, so plotted, was a smooth function of the jet strength S. The exception was the jet at 45°. At a jet strength between

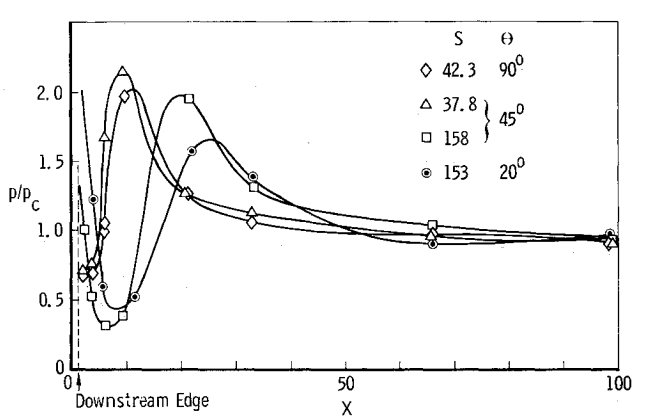

Fig. 4 Surface pressure downstream of shallow, near-normal and transitional jets.

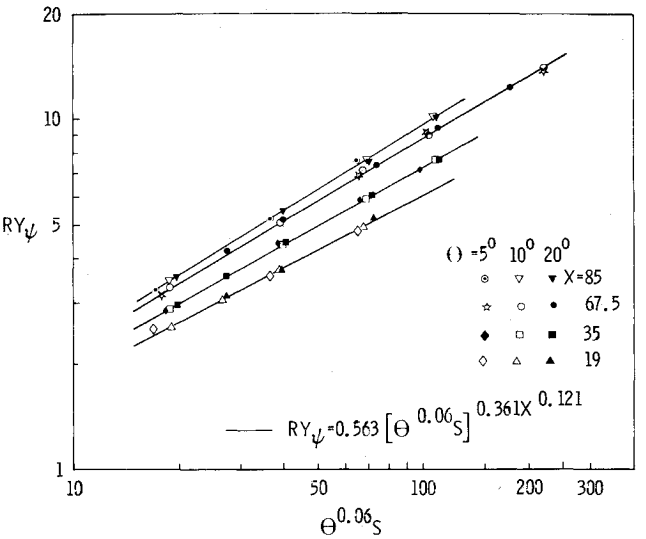

Fig. 5 Correlation of the dividing streamline displacement for shallow jets.

$S = 112$ and $S = 160$ there was a 10% jump in the dividing streamline displacement measured at three different axial stations. A corresponding jump was observed in all other properties measured.

The experimental results for the dividing streamline displacement for the family of shallow jets are shown in Fig. 5. It can be seen that the correlation formula,

$$RY_\psi = 0.563[\theta^{0.06}S]^{0.361X^{0.121}}$$

is a good representation of the measurements for $15 < S < 250$ for $\theta = 5°$, 10° and 20°, and clearly shows the low sensitivity of the dividing streamline displacement to the jet angle.

The measurements for the near-normal jets can be similarly represented by a formula of the type

$$RY_\psi = K(S/S_o)^{aX^n}$$

The function

$$RY_\psi = 1.49[0.143S]^{0.502X^{0.115}} \quad (\theta = 90°)$$

describes the measurements for the jet at $\theta = 90°$, and similarly

$$RY_\psi = 1.39[0.167S]^{0.531X^{0.106}} \quad (\theta = 120°)$$

was found to correlate the measurements for the jet at $\theta = 120°$.[1] In contrast, the results for the transitional jet at 45° can not be represented this way. The expression

$$RY_\psi = 0.231[X^{0.275}S]^{0.650} \quad (\theta = 45°)$$

was found to represent the results up to a jet strength of $S = 112$. These formulae can be used in place of the actual measurements, since the correlations are generally good to within the measurement accuracy.

The penetration of the jets at various angles are compared at the one axial station $X = 67.5$, in Fig. 6. The distinction between the shallow jets, the near-normal jets, and the transitional behavior of the jet at 45° is clearly seen in this figure. The displacement is seen to be a very weak function of the jet angle at small angles, and the exponent of S is the same ($n = 0.60$) for $\theta = 5°$, 10°, and 20°. The displacement of the jets at 90° and 120° depends on S to a higher power ($n = 0.82$), while the jet at 45° follows a power slightly greater than for the shallow jets ($n = 0.65$) and at a higher level.

Two simple limiting one-dimensional expansion processes can be considered in order to examine their pressure dependence. First, consider an isentropic expansion (and turning) of the jet to the cone surface pressure. The expected displacement of the dividing streamline, y_ψ, is given by

$$\frac{A_j^*}{(2ry_{\psi_{is}} + y_{\psi_{is}})\pi} = \Gamma S^{-(\gamma+1/2\gamma)}\left[(S^{\gamma-1/\gamma} - 1)\left(\frac{2}{\gamma-1}\right)\right]^{\frac{1}{2}}$$

Using this expression $RY_{\psi_{is}}$ was evaluated as a function of S for $X = 67.5$, and the result is the lower broken line in Fig. 6. The pressure dependence of this equation and the curves representing the shallow jets, which contain only weak oblique shock waves in their structure are seen to be similar.

Next consider a one-dimensional process which consists of an isentropic expansion of the jet to a normal shock wave, followed by an isentropic expansion (and turning) to the cone surface pressure. This is a simple approximation of the structure observed in the near-normal jets. The Mach number at which the normal shock wave occurs is specified by requiring that the pressure behind the wave is equal to the "plateau pressure" in the separated region ahead of the jet. This is consistent with the observation of jets expanding into still air,[11] and was suggested independently by Shetz[12] for round jets. The plateau pressure, p_{pl} for fully turbulent boundary layers at high Mach number is given by,[13]

$$p_{pl}/p_c = 1 + 0.7\left(0.13M_c^2 - 1.5 + \frac{9.1}{M_c}\right)$$

For the present case, with $M_c = 5.58$ this becomes

$$p_{pl}/p_j = 3.73/S$$

Using this relationship, the Mach number upstream (−) and downstream (+) of the normal shock were obtained as a function of S from Tables.[14] Then

$$(2ry_{\psi_{n.s.}} + y^2_{\psi_{n.s.}})\pi = (A/A^*)_{n.s.+}(p^t_{n.s.-}/p^t_{n.s.+})A^*$$

was used to evaluate RY_ψ as a function of S at $X = 67.5$. The result is the upper broken line in Fig. 6, which shows a pressure dependence close to that of the near normal jets.

Internal Jet Shock Position and Upstream Separation

Previous studies of planar interactions between jets and free-stream have exploited the concept of the "equivalent step height" of the jet, and the investigations have centered about relating the flow parameters to this step height.[3]

It is of interest to compare two characteristic jet heights for various jet angles. The normalized separation height Y_{sep} was obtained from measurements scaled from shadowgraph pictures. The angle of the upstream separation shock wave, Ω, and the distance from the point of intersection of the shock wave with the surface to the upstream edge of the jet, l_{sep}, were scaled from all shadowgraphs taken of the 45°, 90°, and 120° jets. Y_{sep} was calculated assuming that a two-dimensional ramp-like separation occurs, so that from oblique shock analysis

$$\cot\delta = \tan\theta\{[(\gamma + 1/2)M_c^2/M_c^2\sin^2\theta - 1] - 1\}$$

$$Y_{sep} = y_{sep}/h_j = \frac{l_{sep}}{h_j\cos\delta}$$

The displacement of the normal shock in the jet structure from the cone surface, $y_{n.s.}$, was scaled from schlieren photographs. Both Y_{sep} and $Y_{n.s.}$ are shown as a function of the jet strength in Fig. 7. The mean value of the measurement of Y_{sep} and the extreme high and low values obtained from a number of photographs (up to 14) are indicated. The extent of this spread is partly due to the difficulty of scaling from photographs, and partly due to unsteadiness of the flowfield. The fluctuations were evident in the measurements of l_{sep}, which at $\theta = 120°$ and large S varied by as much as one to two boundary-layer thicknesses. The fluctuations were smaller at $\theta = 90°$, and smaller still at $\theta = 45°$.

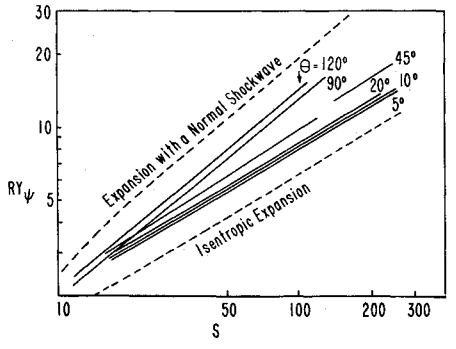

Fig. 6 Dividing streamline displacement measured at $X = 67.5$.

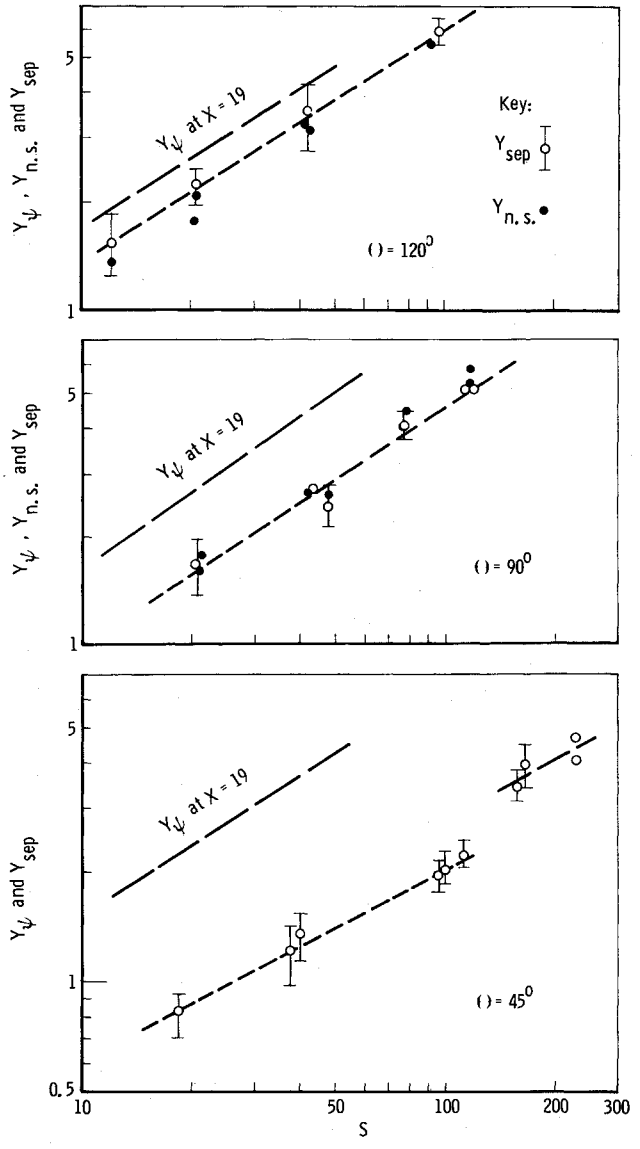

Fig. 7 Dividing streamline displacement in comparison with transverse scales based on upstream separation and internal shock wave position.

In Fig. 7 these two scales are compared with the dividing streamline displacement at the most upstream station at which it was measured. Referring first to the 90° case, $y_{n.s.}$ and y_{sep} are almost equal in value over the range of the measurements. Because of the limited data, the dependence of these scales on the jet strength can not be distinguished as being different from the dependence of the dividing streamline displacement. However, the dividing streamline displacement at this station is approximately 70° greater than the normal shock displacement at the jet. For the jet at 120°, Y_ψ is only 20% greater than Y_{sep}, and 30% greater than $Y_{n.s.}$ approximately.

The dividing streamline penetrates even further compared to the upstream separation scale in the case of the jet at 45°. $Y_\psi \approx 3.5Y_{sep}$ and the dividing streamline has a stronger dependence on the jet strength. The basic change in the flowfield observed in the static pressure and probe measurements with this jet between $S = 110$ and 160 is even more pronounced in the measurements of the separation scale height. The change in the scale of the upstream separation is about 30% in this transition region.

Edge of the Mixing Layer and the Total Jet Displacement

The edge of the mixing layer was defined as the point in the probe traverse where the local stagnation temperature fell to 98% of the freestream value. This procedure was considered acceptable because of the smoothness of the stagnation temperature profiles.[1] While it must be agreed that a certain degree of uncertainty is introduced by the use of such a technique, it was considered the most accurate available for an air–air system. Note also that the value for Y_e was computer selected from the data, thereby reducing judgement errors.

The dividing streamline is a measure of the displacement effect of the jet on the outer flow. However, the total displacement effect is greater than just the displacement of the dividing streamline because of the effect of turbulent shear in the mixing layer outside the dividing streamline. An upper estimate of this effect can be obtained by evaluating the displacement thickness of the flow between the dividing streamline and the edge of the mixing layer and comparing it to Y_ψ. The additional displacement, in the axisymmetric geometry,[1] is given by

$$\delta^* = \int_{y_\psi}^{y_e} 1 - \left(\frac{\rho u}{\rho_e u_e}\right)\left(\frac{r_c + y}{r_c + y_\psi}\right) dy$$

Using the above formula for δ^*, $\Delta/y_\psi = 1 + \delta^*/y_\psi$ was evaluated for each test and the results are shown for $X = 67.5$ in Fig. 8. It can be seen that at $S > 20$ for the shallow jets and the jet at 45°, the total displacement of the outer flow by the jet is described to within 18% by the dividing streamline. The description is even more accurate for smaller values of X, up to the recompression shock wave. For the near normal jets at $S > 20$, the total displacement is up to 30% greater than the dividing streamline displacement, the percentage decreases as S increases. The highly curved injection shock waves associated with the near-normal jets are responsible for the larger values of Δ/y_ψ.

Entrainment and Mixing

The total mass of tunnel air entrained into the jet up to the measurement station, $\dot{m}_{en}$, is given by

$$\dot{m}_{en}/\dot{m}_j = \dot{M}/\dot{m}_j - \dot{m}_{bl}/\dot{m}_j - 1$$

where

$$\dot{M} = 2\pi \int_0^{y_e} \rho \, \text{urdy}$$

and $\dot{m}_{bl}$ is the mass flow contained in the cone boundary layer approaching the jet. The results obtained at $X = 67.5$ are shown in Fig. 9 for $S = 100$, for which $\dot{m}_{bl} \approx 0.1\,\dot{m}_j$. For all jet angles, the entrained mass flow at first remains nearly constant with increasing jet strength, with resultant decrease in the ratio of entrained mass flow to jet mass flow. This is in agreement with the recent findings reported in Ref. 15. At higher jet strengths, the ratio of entrained to jet mass flow passes through a minimum and

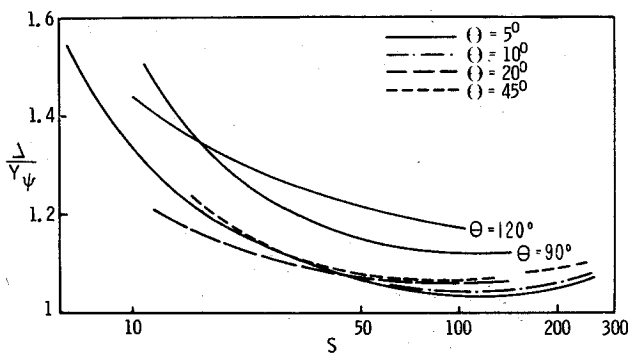

Fig. 8 Dividing streamline displacement in comparison to the total jet displacement.

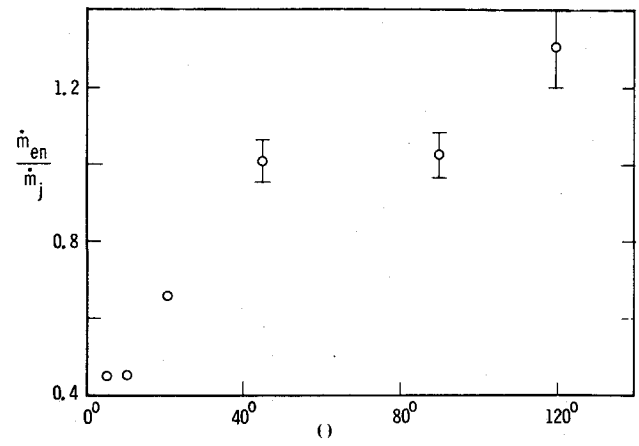

Fig. 9 Measurements of total entrainment at $X = 67.5$ for $S = 100$.

rises with increasing jet strength for the shallow jets and the 45° jet.

The step-like upstream separation of the 45° jet and near-normal jets gives rise to much larger entrainment values. The jet at 45° and the 90° jet have comparable entrainment at high-jet strengths, even though the 45° jet appears as one of a family of shallow jets in a plot of $\dot{m}_{en}$ vs S.[1]

Conclusions

In this investigation of the axisymmetric interaction of a cold surface jet with a heated hypersonic flow, measurements have been made for a range of initial jet angles and jet pressures which suggest that a particular physical view be adopted: namely, that the interaction be considered as a process of expansion from a source, under particular constraints. An analysis which will predict the basic scales of the flowfield in general must account for four important constraints. It must include representations of 1) the pressure induced along the dividing streamline (which is determined by the outer hypersonic flow); 2) the separation behavior upstream of the jet; 3) the separation behavior downstream of the jet; and, 4) the heating of the jet by turbulent mass exchange.

The basic transverse scale investigated here was the dividing streamline, which was identified experimentally using a mass balance. It was found that downstream of the interaction shock structure the dividing streamline displacement was a first-order measure of the displacement effect of the injected fluid for most conditions in the investigation; namely, when the jet dimension was of the order of the boundary-layer thickness, and when the jet was underexpanded.

The displacement of the dividing streamline was found to increase with the angle of the jet and to obey a power law of the form

$$RY_\psi = K(S/S_0)^{aX^n}$$

where K, a, and n are constants, very closely at all jet angles measured except one. The transitional case of the jet at 45° was accurately described by the equation

$$RY_\psi = 0.231[X^{0.275}S]^{0.650}$$

up to a jet strength at which the jet became attached to the downstream surface. The latter transition in structure was accompanied by an increase in the level of all measured properties but was not detected optically as being a discontinuity. With this possible exception, all changes in the flowfield occurred smoothly at all initial jet angles as the jet strength was increased.

The jet at 45° was an exception to the grouping of the jets into families. In the downstream transition, however, it showed the connection between those families. At small jet angles, the dividing streamline had low sensitivity to the jet angle. Qualitatively the 5°, 10°, and 20° jets, which were termed "shallow jets"

were observed to have similar structures near to the jet exit at corresponding jet strengths.

At large jet angles, for which large regions of separated flow occurred both upstream and downstream of the jet and strong shock waves occurred in the jet structure, similar expressions were found to describe the dividing streamline.

Conclusions regarding the entrainment properties of the jets must be considered somewhat tentative because of the difficulty discussed in the text of precisely determining the jet edge. However, within such accuracy limitations, the measurements of mass entrainment into the surface jet indicated that the upstream separated region was a controlling factor. The entrained mass flux was much greater for the near-normal jets than for the shallow jets. The upstream angle of $\theta = 120°$, which gave the greatest dividing streamline displacement also produced the greatest entrainment. However, the jet at 45° at high pressures produced entrainment equal to the jet at 90°. It is suggested that jets at intermediate angles which produce a large region of upstream separation while remaining attached to the surface downstream, hold promise for advanced propulsion applications. The penetration of the jet is less; however, the mass entrained can be comparable and the total momentum of the mixed flow considerably greater than for a corresponding jet normal to the surface. The low-entrainment values and extended cooling lengths exhibited by the shallow jet suggest their use for heat-transfer alleviation at high Mach numbers.

No unsteady flow was detected in the case of the shallow jets. As the jet strength increased, changes in the structure, including the appearance of an upstream region of separation, occurred smoothly. Unsteady flow increased with jet angle and jet strength for the jets with detached injection shock waves and associated upstream separation. The amplitude of the motion of the upstream separation point was about equal to the boundary-layer thickness at the most extreme condition.

The static pressure measurements were useful in interpreting the flow structure but were unsufficiently detailed to provide accurate side force measurements. However, the surface pressure well downstream (~ 100 initial jet widths) was found to decrease below the undisturbed cone value as the jet strength was increased. The slow readjustment of the surface pressure was characteristic of all jet angles. Closer to the jet, significant regions of overpressure occur which can result in positive net side forces, particularly at low-injection pressure.

The method which was used to obtain the distribution of mass flux was an innovation of the present work. The key elements were a fine-wire thermocouple probe[9] which did not require calibration, and the recognition that the mass flux evaluated from stagnation temperature and impact pressure measurements were insensitive to the static pressure.[1] The method has been used successfully to determine properties of a highly complex interaction between two flows. It could become a useful tool for the investigation of mixing at high Mach number.

References

[1] Shreeve, R. P., "An Investigation of a Supersonic Surface Jet—Hypersonic Flow Interaction with Axial Symmetry," Ph.D. thesis, 1970, University of Washington, Seattle, Wash; also, available as Boeing document D1-82-0999, Sept. 1970, Seattle, Wash.

[2] Sterrett, J. R., Barber, J. B., Alston, D. W., and Romeo, D. J., "Experimental Investigation of Secondary Jets from Two-Dimensional Nozzles with Various Exit Mach Numbers for Hypersonic Control Applications," TN D3795, Jan. 1967, NASA.

[3] Werle, M. J., "A Critical Review of Analytical Methods for Estimating Control Forces Produced by Secondary Injection," NOL TR 68-5, Jan. 1968, Naval Ordinance Lab., Pasadena, Calif.

[4] Ferri, A. and Fox, H., "Analysis of Fluid Dynamics of Supersonic Combustion Controlled by Mixing," *Proceedings of the Twelfth Symposium on Combustion*, The Combustion Institute, 1969, pp. 1105–1113.

[5] Kuchemann, D., "Some General Aspects of the Interactions between the Means of Propulsion and Lifting Bodies at Hypersonic Speeds," RAE Tech. Memo Aero. 916, 1966, Euromech 3 Colloquium, Aachen, Germany.

[6] Finley, P. J., "The Flow of a Jet from a Body Opposing a Supersonic Free Stream," *Journal of Fluid Mechanics*, Vol. 26, Part 2, 1966, pp. 337–368.

[7] Simpkins, P. G., "Hypersonic Interactions about a Slender Cone Induced by Radial Mass Injection," Paper 17, AGARD Conference Proceedings 30. Specialists Meeting of the Fluid Dynamics Panel of AGARD, London, England, May 1–3, 1968.

[8] Parthasarathy, K. and Zakkay, V., "Turbulent Slot Injection Studies at Mach 6," ARL 69-0066, April 1969; also, AD 692503.

[9] Shreeve, R. P. and Peecher, D. W., "Stagnation Temperature Measurements at High Mach Number Using Very Small Probes," Boeing document D1-82-0945, Jan. 1970, Seattle, Wash.

[10] Stewartson, K., "The Theory of Laminar Boundary Layers in Compressible Fluids," *Oxford Mathematical Monographs*, Oxford University Press, London, 1964, pp. 104.

[11] Adamson, T. C., Jr. and Nicholls, J. A., "On the Structure of Jets from Highly Underexpanded Nozzles into Still Air," *Journal of the Astronautical Sciences*, Vol. 26, No. 1, 1959, pp. 16–24.

[12] Shetz, J. Z. et al., "Structure of Highly Underexpanded Transverse Jets in a Supersonic Stream," *AIAA Journal*, Vol. 5, No. 5, May 1967, pp. 882–884.

[13] Sterrett, L. R. and Emery, J. C., "Extension of Boundary Layer Separation Criteria to a Mach Number of 6.5 by Utilizing Flat Plates with Forward Facing Steps," TN D618, Dec. 1960, NASA.

[14] Ames Research Staff, "Equations, Tables, and Charts for Compressible Flow," Rep. 1135, 1953, NACA.

[15] Cohen, L. S., Coulter, L. J., and Egan, W. J., Jr., "Penetration and Mixing of Multiple Gas Jets Subjected to Cross Flow," *AIAA Journal*, Vol. 9, No. 4, April 1971, pp. 718–724.